Available at
www.ComputerScienceWeb.com
POWERED BY SCIENCE DIRECT®

ELSEVIER

Neurocomputing 52–54 (2003) 481–487

NEUROCOMPUTING

www.elsevier.com/locate/neucom

Temporal dynamics of attention-modulated neuronal synchronization in macaque V4

Hualou Liang[a,*], Steven L. Bressler[b], Mingzhou Ding[b], Robert Desimone[c], Pascal Fries[d]

[a] *School of Health Information Sciences, University of Texas Health Science Center at Houston, Houston, TX, 77030, USA*

[b] *Center for Complex Systems and Brain Sciences, Florida Atlantic University, Boca Raton, FL 33431, USA*

[c] *Laboratory of Neuropsychology, National Institute of Mental Health, National Institutes of Health, Bethesda, MD 20892, USA*

[d] *F.C. Donders Centre for Cognitive Neuroimaging, University of Nijmegen, 6525 EK Nijmegen, The Netherlands*

Abstract

It was recently observed that neurons in area V4 exhibited enhanced gamma band (35–90 Hz) synchronization when monkeys attended to a visual stimulus as compared to when they were not attending to the same stimulus (Science 291 (2001) 1560). Spike-triggered averaging of local field potentials (LFPs) was used to show attentional modulation in an early period from 50 to 150 ms after stimulus onset (Science 291 (2001) 1560). In this work we further studied the fine temporal structure in the same data by focusing only on the LFPs without reference to the concurrent spike trains. With the method of adaptive multivariate autoregressive (AMVAR) modeling, we discovered that attentional modulation of gamma power (~65 Hz) in V4 can be as brief as about 25 ms. Gamma coherence between two V4 recording sites revealed similar attention effects, as well as a second peak around 45 Hz. Directional influences between two V4 populations revealed that one can play a more dominant role than another. These results implicate gamma oscillation as a possible agent in carrying out attention-biased competition among visual stimuli in favor of those that are behaviorally relevant. The AMVAR method was instrumental in revealing the dynamics of gamma frequency synchronization with high temporal and frequency resolution.

Keywords: Selective visual attention; Multivariate autoregressive modeling; Gamma synchronization; Coherence; Bottom-up; Top-down

* Corresponding author. Tel.: 713-500-3914; fax: 713-500-3915.
E-mail addresses: hualou.liang@uth.tmc.edu (H. Liang).

0925-2312/03/$ - see front matter © 2003 Elsevier Science B.V. All rights reserved.
doi:10.1016/S0925-2312(02)00741-5

1. Introduction

Selective visual attention is the process whereby a particular visual stimulus is selected from multiple stimuli for further processing. In this process, attention biases competition among visual stimuli in favor of those that are most behaviorally relevant [1]. Recent work shows that gamma band (35–90 Hz) synchronization among neurons in cortical area V4 may play a role in this mechanism [3] through elevation of the level of population synchrony in response to the attended stimulus. By applying the technique of spike-triggered averaging to local field potentials (LFPs) it was determined that attentional modulation is already present from 50 to 150 ms poststimulus [3]. Since spike-triggered averaging treats every spike inside the 100 ms interval on an equal footing, the fine temporal dynamics of synchronization in that 100 ms interval is not clear, which the earlier analysis did not attempt to further resolve. Here, we explore the possible finer dynamics in the LFP data related to attention deployment by a parametric spectral analysis method referred to as adaptive multivariate autoregressive (AMVAR) modeling [2].

LFPs from four closely spaced electrodes in area V4 were simultaneously recorded from two macaque monkeys trained to perform a visual spatial attention task. As the monkey fixated centrally, two patches of moving high contrast square wave grating were presented at equal eccentricity, one inside and one outside the receptive field (RF) of the recorded neurons. On different trials, the monkey was cued to attend to one or the other stimulus location. The result was two attention conditions: attention inside the RF vs. attention outside the RF. The analysis described here used 300 correctly performed trials in each attention condition from one monkey.

Local field potential recordings were analyzed to determine power, coherence, and directed transfer function (DTF), a statistical measure of directional influence between two given recordings spectra, derived from AMVAR models. The particular focus was on the detailed time course of attention-modulated neuronal synchronization.

2. Methods

We begin by recapitulating the AMVAR modeling technique introduced in [2] and describe the spectral quantities used in this study.

In MVAR modeling, after an analysis window is chosen LFPs are assumed to be the output of linear filters fed by white noises processes. Thus the p LFP recordings, $\mathbf{X}_t=(x_{1t},x_{2t},\ldots,x_{pt})^{\mathrm{T}}$, can be modeled as AR processes of unknown coefficients, which are given by

$$\sum_{k=0}^{m}\mathbf{A}_k\mathbf{X}_{t-k}=\mathbf{E}_t,$$

where $\mathbf{E}_t$ is a temporally uncorrelated residual error with covariance matrix Σ, and $\mathbf{A}_k$ are $p\times p$ coefficient matrices which are obtained by solving the multivariate Yule–Walker Eq. (of size mp^2) using the Levinson, Wiggins and Robinson (LWR) algorithm [8]. The model order m is determined by the Akaike information criterion (AIC) [7].

Data from multiple trials are treated as realizations of the same underlying (approximately) stationary stochastic process and are combined to produce the estimation of the model coefficients. The term Adaptive means that the above procedure is repeated for each analysis window along the time course of the experiment.

Once the model coefficients $\mathbf{A}_k$ and Σ are estimated, the spectral matrix can be written as

$$S(f) = \langle X(f)X^*(f)\rangle = H(f)\Sigma H^*(f),$$

where the asterisk denotes matrix transposition and complex conjugation, and $H(f) = (\sum_{j=0}^{m} A(j)\mathrm{e}^{-2\pi ijf})^{-1}$ is the transfer function of the system. A suite of tools for spectral analysis can be derived from the spectral matrix [4]. For the purpose of this article, we will only consider the power, coherence, and DTF spectra.

The power spectrum of channel l is given by $S_{ll}(f)$ which is the lth diagonal element of the spectral matrix $S(f)$. The coherence spectrum between channel l and channel k is given by

$$C_{lk}(f) = |S_{lk}(f)|/(S_{ll}(f)S_{kk}(f))^{1/2}.$$

The value of coherence can range from 1, indicating maximum interdependence between channel l and channel k at frequency f, down to 0, indicating no interdependence. The DTF [5] is defined as: $\gamma_{kl} = |H_{kl}(f)|^2$, which measures the statistical influence (information flow) from channel l to channel k. Applications of DTF on cortical field potential time series have shown promise for understanding information transfer between cortical areas [6].

AMVAR analysis was performed with a 50-ms-long window (10 time points) that was stepped point by point from 500 ms prestimulus to 500 ms poststimulus. In each window, data from all 300 trials and 4 sites were used to estimate the MVAR model which yielded all the spectral quantities. The result was a time-frequency representation of the neural dynamics. A bootstrap resampling procedure, with a resampling size of 100, was employed to assess the variability of all the spectral quantities.

3. Results

The power spectrum, as the simplest yet most used measure, reveals how the activity at a site is distributed in frequency with peaks, if any, indicating synchronous oscillatory activity. An example of time-frequency power spectrum from one V4 site (Fig. 1, left) for attention within the RF is used for illustration. At approximately 110 ms poststimulus, there was a brief, narrow-band oscillatory event in the power, peaking around 66 Hz. A similar power spectrum was observed for attention outside the RF condition, but with a lower level of gamma synchronization. This can be clearly seen by taking either the spectrum from the analysis window centered at 110 ms poststimulus (Fig. 1, middle) or power at 66 Hz as a function of time for the two conditions (Fig. 1, right). We see, with great temporal precision, the enhanced gamma synchronization when the monkey directed attention within the RF compared to attention outside the RF, a result consistent with that in [3].

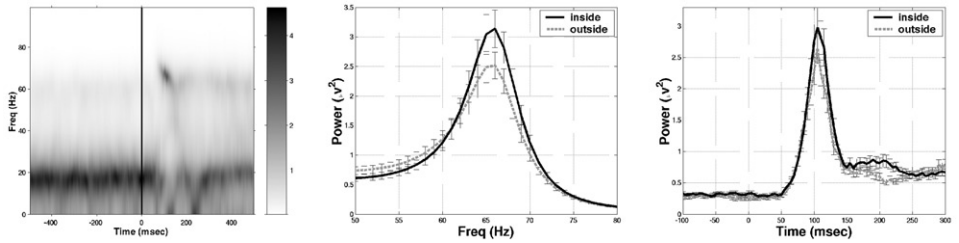

Fig. 1. Left: Time-frequency power plot for V4 recording site 1 for attention inside the RF using a 50-ms (10 point) sliding window. Time 0 indicates the stimulus onset. Middle: Power spectra of site 1 for the two conditions, attention inside the RF (solid lines) and attention outside the RF (dashed lines), from a 50-ms long window centered 110 ms after stimulus onset. Note that both conditions have peaks at 66 Hz, but the peak is larger for the "inside" condition. Right: Power at 66 Hz as a function of time for the two conditions. An initial episode of elevated gamma power related to attention occurred in an interval centered 110 ms poststimulus, lasting about 25 ms, and a second episode of attention modulated gamma power elevation, although at a relatively low overall power level, started around 150 ms poststimulus and lasted around 90 ms. Error bars were obtained by the bootstrap resampling method.

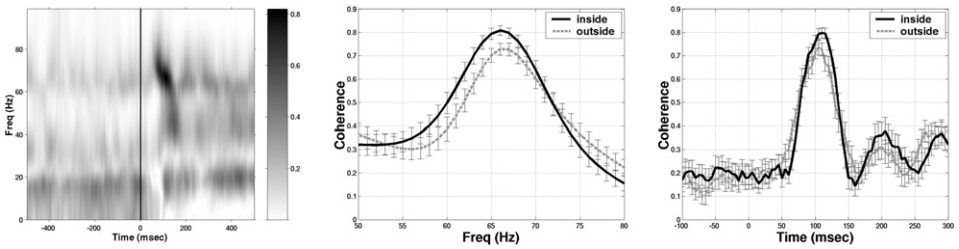

Fig. 2. Left: Time-frequency plot of spectral coherence between V4 recording sites 1 and 2 for attention inside the RF, using a 50-ms (10 point) sliding window. Time 0 indicates the stimulus onset. Middle: Coherence of two conditions, attention inside the RF (solid lines) and attention outside the RF (dashed lines), sliced at 110 ms poststimulus. Note that both conditions have peaks at 66 Hz, but that the peak is larger for the "inside" condition, the same effect as that seen in the power spectra in Fig. 1. Right: Time course of coherence at the peak frequency of 66 Hz for the two conditions. Error bars were obtained by the bootstrap resampling method.

Whereas the power spectrum reflects the activity at a single recording site, the coherence spectrum reflects the functional coupling of neuronal activity between two different sites. An example of time-frequency coherence between the LFPs from two sites for the condition of attention within the RF is shown in Fig. 2 (left). Note that the 66-Hz peak in coherence occurred at approximately the same time and frequency as that seen in the power spectra for site 1 (Fig. 1, left). In addition, a second peak, with a lower coherence, emerged also in the gamma range, near 45 Hz, at a later time. The coherence spectra taken from the analysis window at 110 ms poststimulus for both conditions are shown in Fig. 2 (middle) and the coherence at 66 Hz as a function of time is shown in Fig. 2 (right). At approximately 110 ms poststimulus, the 66-Hz coherence peak is larger for the "inside" condition, an effect similar to that of

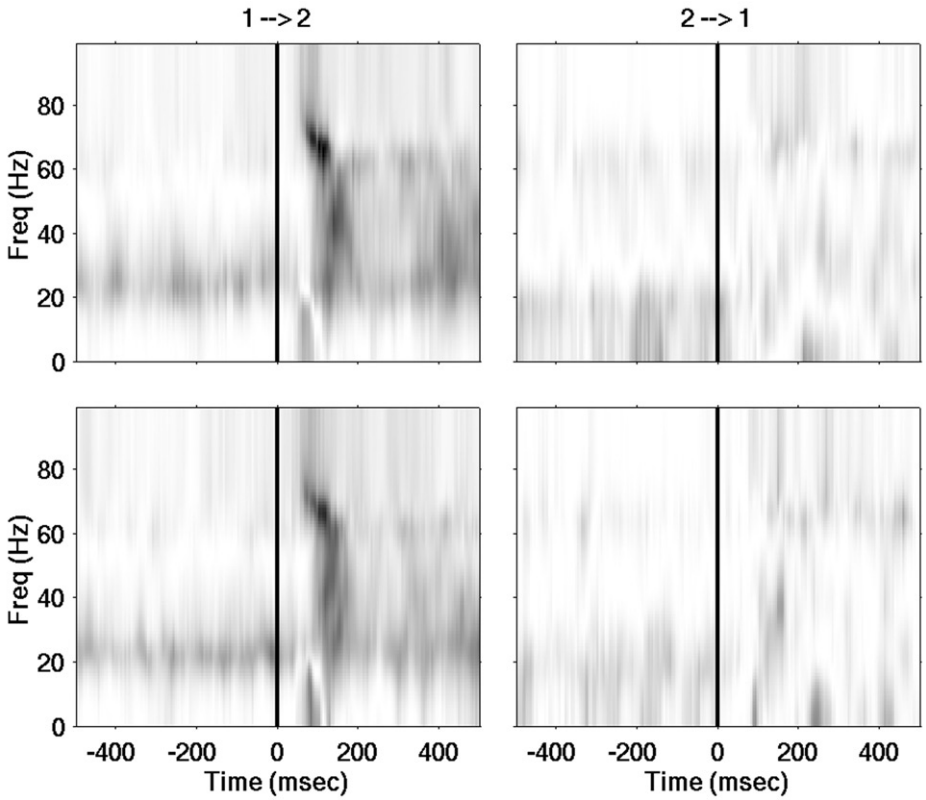

Fig. 3. Time-frequency plots of the DTF between sites 1 and 2 for the two conditions, attention inside the RF (top) and attention outside the RF (bottom), using a 50-ms (10 point) sliding window. DTF values are represented on a color scale from 0 (white) to the maximum value (black). The vertical solid line indicates the stimulus onset.

the power at this frequency (Fig. 1), indicating that attention modulation also affected the coupling between spatially extended V4 ensembles.

The DTF, unlike coherence, is a directional measure of the statistical influence between two processes. Fig. 3 shows two time-frequency plots for each condition: one showing influence from site 1 to 2 (left column), and the other showing the influence from 2 to 1 (right column). In the $1 \rightarrow 2$ plots, we see a pattern similar to the coherence plots for these sites (Fig. 2, left), with the 66- and 45-Hz poststimulus gamma peaks. However, both peaks are largely absent in the reverse ($2 \rightarrow 1$) direction. Therefore, it seems that the 66- and 45-Hz coherences could be attributed to the directional influence from site 1 to site 2.

The time course of DTF for 1 to 2 and from 2 to 1, at 66 Hz for the condition of attention inside the RF is shown in Fig. 4. This pattern suggests that location 1 may drive location 2 with a small, delayed feedback.

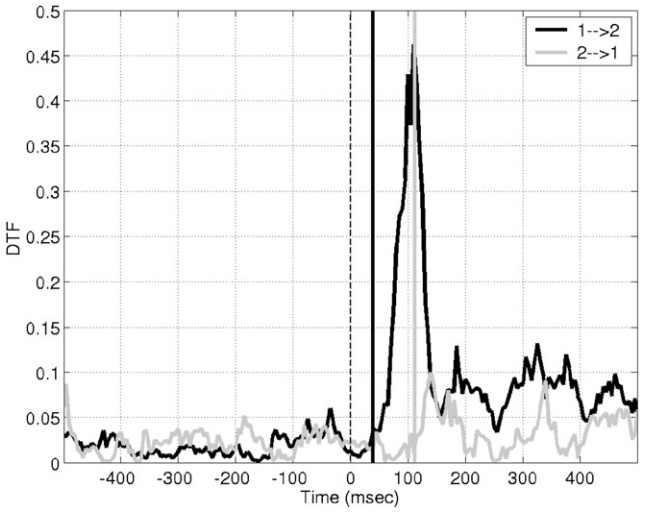

Fig. 4. Time course of DTF at 66 Hz for the "inside" condition. The influence from site 1 to site 2 (black) shows a large peak near 100 ms poststimulus. The onset of this event is marked by the vertical black solid line. The 2-to-1 DTF (gray) shows a much smaller poststimulus increase (marked by the vertical gray line), that is delayed with respect to the 1-to-2 DTF. The vertical dashed line indicates the stimulus onset.

4. Conclusions

In this brief report we examined the temporal structure of attention-modulated neuronal synchronization in macaque area V4 by AMVAR spectral analysis, and found that gamma power ($\sim$65 Hz) was elevated when attention was directed to a stimulus within the RF of the neurons at a recording site. We also found elevated LFP coherence in the gamma frequency range due to attention at the same gamma peak frequency, as well as at a second gamma peak ($\sim$45 Hz) frequency, among a subset of recording sites. Directional influences between two V4 subpopulations revealed that one direction was more dominant than the other for these two gamma-frequency events. Overall, these results, combined with the recent idea that heightened levels of synchrony among multiple pre-synaptic spike trains increase their post-synaptic efficacy on target neurons, suggest a possible mechanism concerning how attention biases competition among visual stimuli in favor of those that are behaviorally relevant [1].

This report, although preliminary, suggests that the AMVAR methodology, together with the accompanying set of spectral quantities such as power, coherence and DTF, provides a useful tool with high temporal and frequency resolution for characterizing functional relations among neural ensembles during visual selective attention tasks. Currently, the analysis is being expanded to systematically assess the precise timing of attention modulation in the gamma range and other quantitative information from all the recordings sites for all sessions from all monkeys.

Acknowledgements

S.L.B. and M.D. are supported by NSF grant IBN0090717, NIMH grants MH58190 and MH42900, and ONR grant N00014-99-1.

References

[1] R. Desimone, J. Duncan, Neural mechanisms of selective visual-attention, Annu. Rev. Neurosci. 18 (1995) 193–222.
[2] M. Ding, S.L. Bressler, W. Yang, H. Liang, Spectral analysis of cortical event-related potentials by adaptive multivariate autoregressive modeling: model order, stability and consistency, Biol. Cybernet. 83 (2000) 35–45.
[3] P. Fries, J.H. Reynolds, A.E. Rorie, R. Desimone, Modulation of oscillatory neuronal synchronization by selective visual attention, Science 291 (2001) 1560–1563.
[4] G.M. Jenkins, D.G. Watts, Spectral Analysis and its Applications, Holden Day, San Francisco, 1968.
[5] M.J. Kaminski, K.J. Blinowska, A new method of the description of the information flow in the brain structures, Biol. Cybernet. 65 (1991) 203–210.
[6] H. Liang, M. Ding, R. Nakamura, S.L. Bressler, Causal influences in primate cerebral cortex during visual pattern discrimination, NeuroReport 11 (2000) 2875–2880.
[7] S.L. Marple, Digital Spectral Analysis with Applications, Prentice-Hall, Englewood Cliffs, NJ, 1987.
[8] M. Morf, A. Vieira, D. Lee, T. Kailath, Recursive multichannel maximum entropy spectral estimation, IEEE Trans. Geosci. Electron. 16 (1978) 85–94.